

# Novel Silicate Anion: $\text{Si}_8\text{O}_{22}^{12-}$ . Hydrothermal Synthesis and X-ray Powder Structure of Three New Niobium Silicates

Miguel A. Salvadó, Pilar Pertierra, and Santiago García-Granda\*

Departamento de Química Física y Analítica, Universidad de Oviedo, 33006 Oviedo, Spain

Sergei A. Khainakov and José R. García\*

Departamento de Química Orgánica e Inorgánica, Universidad de Oviedo, 33006 Oviedo, Spain

Anatoly I. Bortun† and Abraham Clearfield\*

Department of Chemistry, Texas A&M University, College Station, Texas 77843-3255

Received January 29, 2001

A sodium niobium(V) tetrasilicate,  $\text{Na}_2\text{H}(\text{NbO})\text{Si}_4\text{O}_{11}\cdot 1.25\text{H}_2\text{O}$  (**1**), was synthesized hydrothermally at 190 °C from a mixture of silicic acid, NaOH,  $\text{NbCl}_5$ , and  $\text{H}_2\text{O}_2$  and added hydrochloric acid. The successive treatment of **1** with nitric acid yielded  $\text{HNb}(\text{H}_2\text{O})\text{Si}_4\text{O}_{11}\cdot \text{H}_2\text{O}$  (**2**). Contact of **2** with cesium hydroxide solutions converted it to the partially exchanged  $\text{Cs}^+$  phase  $\text{Cs}_{0.66}\text{H}_{0.33}\text{Nb}(\text{H}_2\text{O})\text{Si}_4\text{O}_{11}$  (**3**). The three structures were solved from X-ray powder diffraction data. All compounds crystallize in the monoclinic space group  $P2_1/m$  with  $Z = 2$ , containing the  $\text{Si}_8\text{O}_{22}^{12-}$  anion. This new silicate anion type is related to the  $\text{Si}_4\text{O}_{11}^{6-}$  unit, which is present in the amphibole series. The difference between both anion types lies in the chain periodicity: two for amphiboles or four for the new niobium silicates. These niobium silicates have framework structures enclosing tunnels in which the alkali cations reside.

## Introduction

Recent years have seen an upsurge of interest in the syntheses and characterization of new titanosilicates<sup>1–5</sup> of mixed frameworks built up from  $\text{SiO}_4$  tetrahedra and  $\text{TiO}_6$  octahedra. The silicon and titanium atoms can be replaced by other tetravalent elements: germanium in tetrahedral sites and zirconium, tin, germanium, and lead in octahedral sites.<sup>6–10</sup> Further, pentavalent metals (i.e., niobium) can also occupy the octahedral position. Niobium and tantalum silicates have been studied by Raveau and co-workers,<sup>11,12</sup> who found two structural types,  $\text{A}_3\text{Ta}_6\text{Si}_4\text{O}_{26}$  (A = Ba, Sr) and  $\text{K}_6\text{M}_6\text{Si}_4\text{O}_{26}$  (M = Nb, Ta), with an interesting feature: they contain distorted pentagonal channels.

Our aim was to obtain three-dimensional framework structures offering possibilities for fast alkali ion mobility and/or ion exchange properties. Compounds with covalent networks built from tetrahedral and octahedral polyhedra are extended to other systems containing octahedrally coordinated tin, niobium, and tantalum.<sup>13</sup> Other authors have prepared and characterized novel synthetic materials with structures similar to those of the natural zeolites. Titanium–niobium silicates<sup>14–16</sup> and a new double silicate,  $\text{Rb}_3\text{Nb}_3\text{O}_6[\text{Si}_3\text{O}_9]$ , representative of the pyroxene group,<sup>17</sup> in which the structural cavities contain the large alkali cation, are known. These examples show a wide variety of structure types for the niobium silicates, which is similar to the diversity described for titanosilicates in order to build up different frameworks. Knowledge of the structure makes it possible to study and to modify the ion-exchange properties of these compounds as a function of their chemical composition.<sup>4,18</sup>

These examples show a wide variety of structure types for the niobium silicates, which is similar to the diversity described for titanosilicates in order to build up different frameworks. Knowledge of the structure makes it possible to study and to modify the ion-exchange properties of these compounds as a function of their chemical composition.<sup>4,18</sup>

\* García-Granda e-mail: sgg@saoron.quimica.uniovi.es.

† Actual address: ASEC Delphi Energy & Chassis Systems, 1301 Main Parkway, Catoosa, OK 74015.

- (1) Roberts, M. A.; Sankar, G.; Thomas, J. M.; Jones, R. H.; Du, H.; Chen, J.; Pang, W.; Xu, R. *Nature* **1996**, *381*, 401.
- (2) Serrano, D. P.; Li, H.-X.; Davis, M. E. *J. Chem. Soc., Chem. Commun.* **1992**, 745.
- (3) Anthony, R. G.; Philip, C. V.; Dosch, R. G. *Waste Manage. (Oxford)* **1993**, *13*, 503.
- (4) (a) Poojary, D. M.; Bortun, A. I.; Bortun, L. N.; Clearfield, A. *Inorg. Chem.* **1996**, *35*, 6131. (b) Poojary, D. M.; Cahill, R. A.; Clearfield, A. *Chem. Mater.* **1994**, *6*, 2364.
- (5) Pertierra, P.; Salvadó, M. A.; García-Granda, S.; Bortun, A. I.; Clearfield, A. *Inorg. Chem.* **1999**, *38*, 2563.
- (6) Choisnet, J.; Deschanvres, A.; Raveau, B. *J. Solid State Chem.* **1972**, *209*.
- (7) Brandt, H.-J.; Otto, H. H. Z. *Kristallogr.* **1997**, *212*, 34.
- (8) (a) Cascales, C.; Gutiérrez-Puebla, E.; Monge, M. A.; Ruíz-Valero, C. *Angew. Chem., Int. Ed.* **1998**, *37*, 129. (b) Cascales, C.; Gutiérrez-Puebla, E.; Iglesias, M.; Monge, M. A.; Ruíz-Valero, C. *Angew. Chem., Int. Ed.* **1999**, *38*, 2436.
- (9) Behrens, E. A.; Poojary, D. M.; Clearfield, A. *Chem. Mater.* **1998**, *10*, 959.
- (10) Pertierra, P.; Salvadó, M. A.; García-Granda, S.; Trobajo, C.; García, J. R.; Bortun, A. I.; Clearfield, A. *J. Solid State Chem.* **1999**, *148*, 41.

- (11) Choisnet, J.; Nguyen, N.; Groult, D.; Raveau, B. *Mater. Res. Bull.* **1976**, *11*, 887.
- (12) Choisnet, J.; Nguyen, N.; Raveau, B. *Mater. Res. Bull.* **1977**, *12*, 91.
- (13) Crosnier, M. P.; Guyomard, D.; Verbaere, A.; Piffard, Y.; Tournoux, M. *J. Solid State Chem.* **1992**, *98*, 128.
- (14) Rocha, J.; Brandão, P.; Lin, Z.; Esculcas, A. P.; Ferreira, A.; Anderson, M. W. *J. Phys. Chem.* **1996**, *100*, 14978.
- (15) Rocha, J.; Brandão, P.; Lin, Z.; Kharlamov, A.; Anderson, M. W. *J. Chem. Soc., Chem. Commun.* **1996**, 669.
- (16) Rastsvetaeva, R. K.; Tamazyán, R. A.; Pushcharovskii, D. Y.; Nadezhina, T. N.; Voloshin, A. V. *Crystallogr. Rep.* **1994**, *39*, 908.
- (17) Genkina, E. A.; Belokoneva, E. L.; Mill, B. V.; Butashin, A. V.; Maksimov, B. A. *Sov. Phys. Crystallogr.* **1992**, *37*, 316.
- (18) Nguyen, N.; Studer, F.; Groult, D.; Choisnet, J.; Raveau, B. *J. Solid State Chem.* **1976**, *19*, 369.

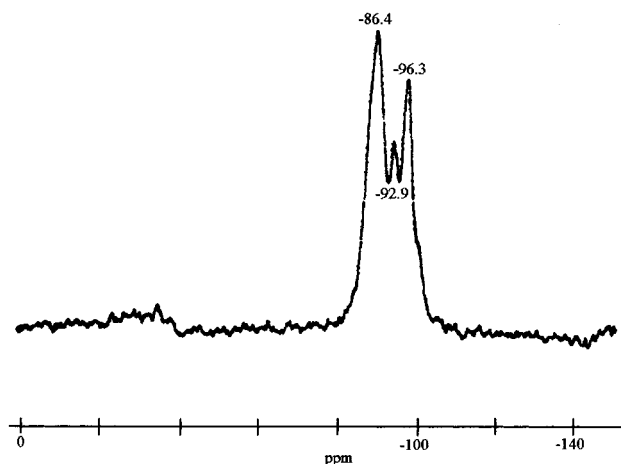


Figure 1.  $^{29}\text{Si}$  MAS NMR for  $\text{Na}_2\text{H}(\text{NbO})\text{Si}_4\text{O}_{11}\cdot 1.25\text{H}_2\text{O}$  (1).

This paper describes the synthesis and structure solution of three new niobium(V) silicates with the niobium atom in octahedral coordination and in which all of the phases contain a novel silicate unit,  $\text{Si}_8\text{O}_{22}^{12-}$ .

### Experimental Section

**Sample Preparation. 1. Na Phase.**  $\text{Na}_2\text{H}(\text{NbO})\text{Si}_4\text{O}_{11}\cdot 1.25\text{H}_2\text{O}$  (1) was synthesized hydrothermally. A silicon-containing solution was prepared by dissolving 6.0 g of silicic acid (62.4 mmol) in 34 mL of 5.9 M NaOH in a 100 mL Teflon beaker. A niobium-containing solution was prepared by adding gradually, with stirring, 4.05 g (15 mmol) of  $\text{NbCl}_5$  to 14 mL of a HCl 6 M solution. After that, 8 mL of 30%  $\text{H}_2\text{O}_2$  was added quickly to the  $\text{NbCl}_5$  in HCl solution. The silicon-containing and niobium-containing solutions were mixed together, and the resultant yellow homogeneous solution was transferred into a 100 mL Teflon lined stainless steel autoclave, which was sealed and treated at 190 °C and autogenous pressure for 12 days. The precipitate formed was filtered, washed with deionized water, and dried at 70 °C in air.

**2. The H phase** of the niobium silicate,  $\text{HNb}(\text{H}_2\text{O})\text{Si}_4\text{O}_{11}\cdot \text{H}_2\text{O}$  (2), was prepared by successive treatment of 1 with 0.2 M  $\text{HNO}_3$  solution ( $V/m$  ratio 200:1, mL/g) for several days at ambient temperature and static conditions. The treatment was finished when no further sodium release was found (AAS control) after sample contact with a fresh portion of acid. The acid form of the niobium silicate was washed with deionized water and dried at 70 °C in air.

**3. The Cs phase** of the niobium silicate,  $\text{Cs}_{0.66}\text{H}_{0.33}\text{Nb}(\text{H}_2\text{O})\text{Si}_4\text{O}_{11}$  (3), was prepared by placing 1 g of the acid form (2) in contact with 400 mL of 0.1 M CsOH solution for 6 days at ambient temperature with periodic shaking. After that, the sample was filtered, washed with 20 mL of deionized water, and dried at 70 °C in air.

**Instrumental Techniques.** Elemental analysis was performed on a Cameca SX-50 electron microprobe equipped with four wavelength-dispersive spectrometers with TAP, PET, and LIF analyzing crystals. Gas-flow proportional counters using P-10 gas (90% argon, 10% methane) were used on all spectrometers. Analyses were conducted at 15 keV accelerating voltage, a beam current of 15 mA, and a beam diameter of 3 mm (counting time was 10 s). Anal. calcd for 1: Na, 9.86; Nb, 19.92; Si, 24.01. Found: Na, 9.6; Nb, 19.8; Si, 24.4. Anal. calcd for 2: Nb, 22.23; Si, 26.80. Found: Nb, 23.3; Si, 27.2. Anal. calcd for 3: Cs, 18.16; Nb, 19.04; Si, 22.96. Found: Cs, 19.9; Nb, 18.5; Si, 21.9. The TG curves were obtained with a Mettler TA4000 (TG 50) thermoanalyzer, employing a heating rate of 10 °C/min. An electron micrograph was recorded with a JEOL JSM 6100 electron microscope operating at 20 kV. The magnetic moment was measured on a Johnson Matthey magnetic susceptibility balance.

**NMR Study.**  $^{29}\text{Si}$  MAS NMR spectra were collected on a Bruker MSL 300 spectrometer. The presence of three peaks with intensity ratio 2:1:2, at -86.4, -92.9, and -96.3 ppm, clearly indicates three different types of silicon atoms in compound 1 (Figure 1).

**X-ray Data Collection.** Powder X-ray diffraction patterns were recorded on a Philips diffractometer using graphite-monochromatic Cu

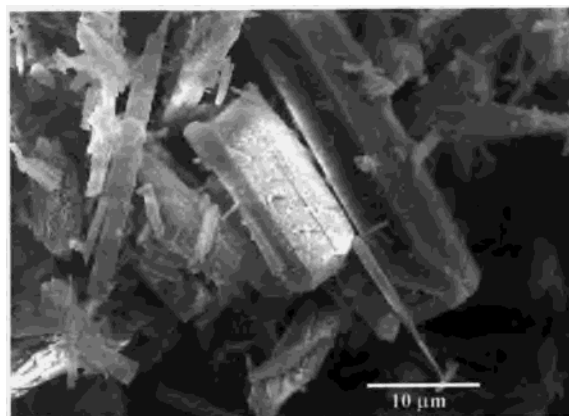


Figure 2. Electron micrograph showing the habit of the crystals of 1.

$\text{K}\alpha$  radiation operating in the Bragg–Brentano ( $\theta/2\theta$ ) geometry. As the micrograph in Figure 2 reveals, the morphology of crystals was a candidate for preferred orientation effects, and this was kept in mind in the subsequent data collection and analysis.

The three samples were gently ground in an agate mortar, mixed with amorphous Cabosil, and side-loaded in order to minimize the preferred orientation. All data were collected at room temperature over the angular range 3–110° for  $2\theta$  with a step size of 0.02° and a count time of 10 s/step.

**Crystal Structure Analysis.** The X-ray powder patterns of the novel niobium silicates were indexed using the program TREOR<sup>19</sup> from 20 low-angle, accurately measured, unambiguous reflection positions. A monoclinic cell was obtained for all the phases. Compound 1:  $a = 7.14(2)$ ,  $b = 9.14(1)$ ,  $c = 8.87(1)$  Å;  $\beta = 101.5(1)^\circ$ . Figures of merit:  $M_{20} = 13^{20}$  and  $F_{20} = 23$  (0.023, 39).<sup>21</sup> Compound 2:  $a = 7.364(2)$ ,  $b = 9.012(4)$ ,  $c = 9.631(2)$  Å;  $\beta = 107.30(2)^\circ$ . Figures of merit:  $M_{20} = 21$  and  $F_{20} = 40$  (0.013, 38). Compound 3:  $a = 7.340(4)$ ,  $b = 9.026(5)$ ,  $c = 9.612(3)$  Å;  $\beta = 106.96(2)^\circ$ . Figures of merit:  $M_{20} = 17$  and  $F_{20} = 26$  (0.019, 41), which is similar to that for the acid form (compound 2).

**Compound 1.** The systematic absences are compatible with the space groups  $P2_1$  and  $P2_1/m$ . Reflection intensities were extracted from the diffraction pattern using the Le Bail method.<sup>22</sup> The centrosymmetric space group was confirmed by subsequent structure solution. 1537  $F^2$  values extracted from the data were used as input for the direct methods program SIRPOW,<sup>23</sup> using the optional instruction PROR in the [101] direction, which accounts for the preferred orientation. The niobium atom, three silicon atoms (which are in agreement with the MAS NMR data), and eight oxygen atoms belonging to the framework were identified. Furthermore, three new atoms outside the network (Wyckoff positions 4f, 2e, and 2c) were located. All of the atomic positions that built up the framework were used as a starting model for the Rietveld refinement in the FULLPROF program.<sup>24</sup> Subsequently, the structure was refined with a sodium cation and an oxygen atom belonging to a water molecule (Wyckoff positions 4f and 2e), but the site occupancies were not clear from the refinement.

Then, the results from elemental analysis were used. The Wyckoff positions 4f, 2e, and 2c were labeled as a sodium cation and two oxygen atoms belonging to water molecules, respectively. The TG curve shows the release of the coordinate water molecules in three steps (Figure 3a): 0.25 mol at 75 °C (labeled O9, Wyckoff position 2c, occupancy 0.5), 1 mol at 225 °C (labeled O10), and finally 0.5 mol at 530 °C, belonging to the oxygen atom of the niobyl group (labeled O3) with

(19) Werner, P.-E.; Eriksson, L.; Westdahl, M. *J. Appl. Crystallogr.* **1985**, *18*, 367.

(20) de Wolff, P. M. *J. Appl. Crystallogr.* **1968**, *1*, 108.

(21) Smith, G. S.; Snyder, R. L. *J. Appl. Crystallogr.* **1979**, *12*, 60.

(22) Le Bail, A.; Duroy, H.; Fourquet, J. L. *Mater. Res. Bull.* **1988**, *23*, 447.

(23) Altomare, A.; Cascarano, G.; Giacovazzo, C.; Guagliardi, A.; Burla, M. C.; Polidori, G.; Camalli, M. *J. Appl. Crystallogr.* **1994**, *27*, 435.

(24) Rodríguez-Carvajal, J. FULLPROF: A Program for Rietveld Refinement and Pattern Matching Analysis. *Abstracts of the Satellite Meeting on Powder Diffraction of the XV Congress of the IUCr*, Toulouse, France, 1990; p 127.

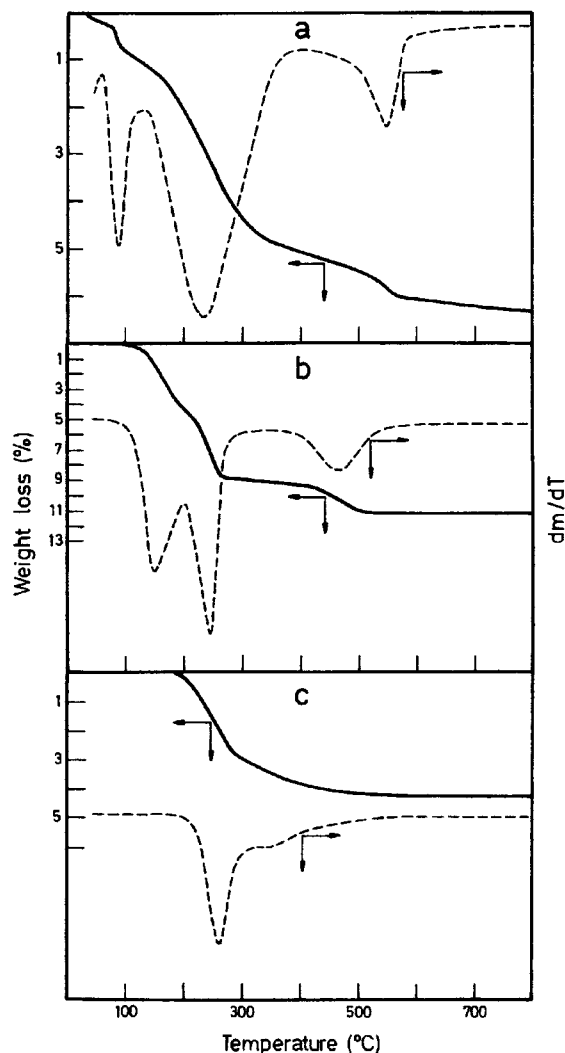


Figure 3. TG (—) and DTG (---) curves of (a) **1**, (b) **2**, and (c) **3**.

the silanol proton. This information was definitive for the identification of all of the atoms outside of the framework and successful performance of the final cycles of the Rietveld refinement.

In the refinement, the temperature factors of each discrete atom type in the framework were constrained to have the same value, but the atoms outside the framework were independently refined. These atoms exhibited higher temperature factors, indicating an easy displacement.

The structure was refined with soft constraints Si–O and Nb–O (1.61(1) and 2.00(1) Å). The peak shapes were described using the split pseudo-Voigt function, to partially accommodate the asymmetric profile shape. A preferred orientation correction along [010] and an additional asymmetry correction at low angles were applied. The refinement of the preferred orientation parameter of the March–Dollase model ( $G_1 = 1.20$ ) shows the presence of the significant orientation of the fiber type in accord with the SEM micrograph. Despite the preferred orientation, the first peak was included in the Rietveld refinement.

The final Rietveld refinement difference plot for compound **1** is given in Figure 4a.

**Compound 2.** Despite the small differences in unit cells, a powder pattern collected in the same conditions on **2** did not refine against the framework structure of **1**. During the course of study, it was found that the data were severely affected by preferred orientation effects to a greater extent than those of phase **1**. To overcome this problem, a sample was prepared by using a tubular aerosol suspension chamber developed by Davis Consulting.<sup>25</sup> Despite this, refinement against the new data was unsuccessful. Therefore, an ab initio structure solution was undertaken. 1644  $F^2$  values were extracted from the profile and

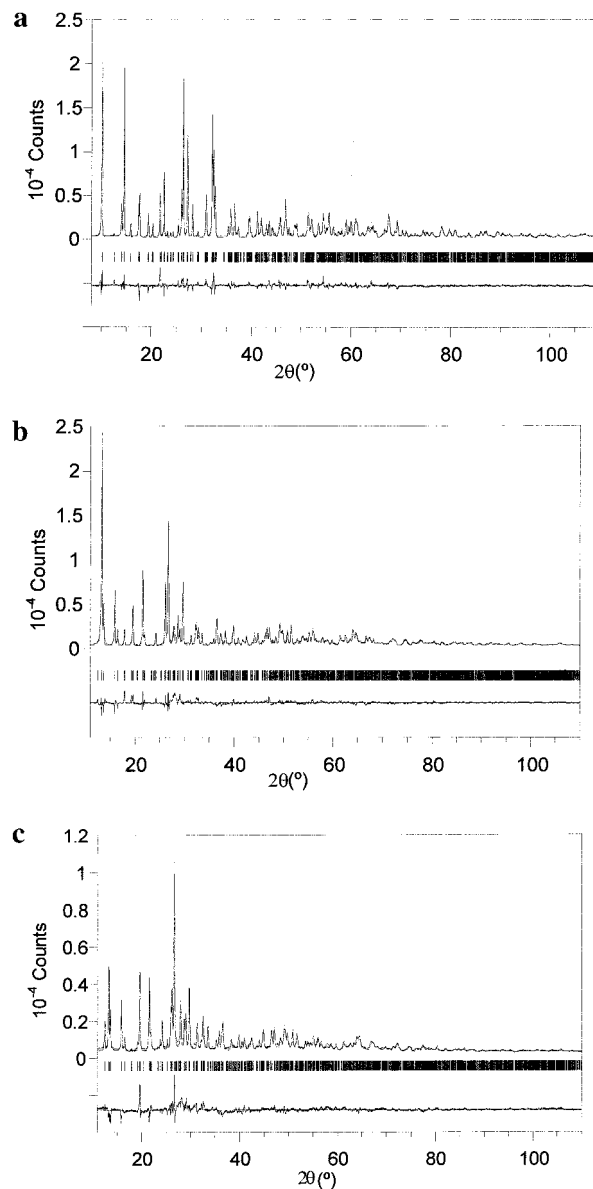


Figure 4. X-ray powder diffraction pattern of (a) **1**, (b) **2**, and (c) **3**. Cross marks correspond to observed data; the solid line is the calculated profile. Tick marks indicate the positions of allowed reflections, and a difference curve, at the same scale, is plotted at the bottom of the pattern.

were used as the input data for the SIRPOW program. Positional atom parameters belonging to a distorted framework were obtained. The geometrical disposition was modeled by geometrical refinement with the DLS-76 program,<sup>26</sup> using distance constraints of Nb–O (2.0 Å) and Si–O (1.61 Å). The unit cell parameters were held fixed. In the modeled structure, the niobium atom shows a distorted octahedral environment. Now, the structure was successfully refined using the initial powder pattern, including a preferred orientation correction ( $G_1 = 1.35$ ). The structure refinement was carried out in a manner similar to that described for compound **1**. A difference Fourier map prepared with SHELX93<sup>27</sup> revealed the position of an oxygen atom (water molecule) outside of the framework.

The TG curve shows the release of the water molecules in three steps (Figure 3b): 1 mol at 150 °C (O9 water molecule), 1 mol at 240 °C (O3 water molecule), and finally 0.5 mol at 460 °C (the silanol

(25) Davis, B. L. *Powder Diff.* **1986**, *1*, 240.

(26) Baerlocher, Ch.; Hepp, A.; Meier, W. M. *DLS-76. A program for the simulation of crystal structures by geometric refinement*; ETH: Zürich, Switzerland, 1977.

(27) Sheldrick, G. M. *SHELXL93. Program for the Refinement of Crystal Structures*; University of Göttingen: Germany, 1993.

**Table 1.** Crystal Data of the Novel Niobium Silicates

|  | 1   | 2  | 3  |
|--|---|--|--|
| formula                                    | Na <sub>2</sub> H(NbO)Si <sub>4</sub> O <sub>11</sub> ·1.25H <sub>2</sub> O | HNb(H <sub>2</sub> O)Si <sub>4</sub> O <sub>11</sub> ·H <sub>2</sub> O | Cs <sub>0.66</sub> H <sub>0.33</sub> Nb(H <sub>2</sub> O)Si <sub>4</sub> O <sub>11</sub> |
| cryst syst                                 | monoclinic  | monoclinic   | monoclinic   |
| space group                                | <i>P</i> 2 <sub>1</sub> / <i>m</i>  | <i>P</i> 2 <sub>1</sub> / <i>m</i>                                     | <i>P</i> 2 <sub>1</sub> / <i>m</i>   |
| <i>Z</i>                                   | 2   | 2  | 2  |
| <i>a</i> (Å)                               | 7.1543(2)   | 7.3639(4)  | 7.3581(5)  |
| <i>b</i> (Å)                               | 9.1228(3)   | 9.0086(7)  | 9.0354(9)  |
| <i>c</i> (Å)                               | 8.8966(3)   | 9.6355(5)  | 9.6377(7)  |
| $\beta$ (deg)                              | 101.341(2)  | 107.293(3)   | 107.019(4)   |
| fw   | 466.75  | 418.28   | 487.31   |
| <i>V</i> (Å <sup>3</sup> )                 | 569.32(2)   | 610.31(7)  | 612.69(9)  |
| $\rho_{\text{calc}}$ (g·cm <sup>-3</sup> ) | 2.72  | 2.28   | 2.64   |
| <i>F</i> (000)                             | 457   | 412  | 463  |
| 2 $\theta$ range (deg)                     | 8–110   | 11–110   | 11–110   |
| step                                       | 0.02  | 0.02   | 0.02   |
| parameters                                 | 60  | 54   | 51   |
| no. soft constraints                       | 11  | 13   | 13   |
| <i>R</i> <sub>wp</sub>                     | 13.3  | 13.4   | 12.0   |
| <i>R</i> <sub>exp</sub>                    | 3.32  | 3.31   | 3.78   |
| $\chi^2$                                   | 15.9  | 16.5   | 10.0   |
| <i>R</i> <sub>B</sub>                      | 9.55  | 11.0   | 15.4   |

proton). The final Rietveld refinement difference plot for compound **2** is given in Figure 4b.

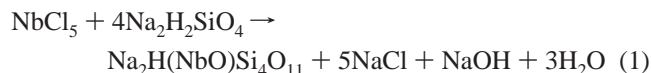
**Compound 3.** The coordinates of structure **2** were used as a starting model for the Rietveld refinement of the full pattern. After the initial refinement of scale, background function, and unit cell parameters, the atomic positions were refined with the previously mentioned soft constraints. The structure refinement was carried out in a manner similar to that described for previous compounds. The value of the preferred orientation correction was  $G_1 = 1.31$ . Also, the first peak, being severely affected by preferred orientation, was not included in the refinement. A difference Fourier map revealed the position of the Cs atom at (0,0,1/2), and the occupancy was fixed according to the elemental analysis data. The final Rietveld refinement difference plot for compound **3** is given in Figure 4c.

The TG curve shows the release of the coordinate water molecules in two steps (Figure 3c): 1 mol at 260 °C (O3 water molecule) and 0.17 mol at 350 °C (corresponding to 0.33 not exchanged protons).

Crystallographic and experimental parameters are given in Table 1, final positional and thermal parameters in Tables 2, 4, and 6, and bond lengths and angles in Tables 3, 5, and 7, for **1**, **2**, and **3**, respectively. Descriptions of distances between atoms in the channels of all three compounds can be found in Table 8.

## Results and Discussion

The reaction to produce phase **1** may be represented by eq 1.



The studied crystal structures are built up from NbO<sub>6</sub> octahedra and SiO<sub>4</sub> tetrahedra. There are Si–O–Si and Si–O–Nb bonds, but no Nb–O–Nb bonds. The octahedral coordination around the niobium atom is completed with an oxygen atom (O3), which is not linked to a silicon atom. In structure **1**, this oxygen atom exhibited a shorter distance than the rest of the oxygen atoms, 1.66(1) Å, which is in agreement with the presence of a niobyl group.<sup>13,28,29</sup> The longer distances found for this oxygen atom in the other two phases are probably due to the presence of a water molecule.<sup>30</sup> The stoichiometric formula supports the presence of the Si<sub>4</sub>O<sub>11</sub><sup>6-</sup> anion (for each niobium atom per unit formula), although the cell contents are better described as

**Table 2.** Fractional Atomic Coordinates and Isotropic Displacement Parameters (Å<sup>2</sup>) for Na<sub>2</sub>H(NbO)Si<sub>4</sub>O<sub>11</sub>·1.25H<sub>2</sub>O

| atom              | Wyckoff position | <i>x</i>  | <i>y</i>  | <i>z</i>  | <i>B</i> |
|-------------------|------------------|-----------|-----------|-----------|----------|
| Nb                | 2e               | 0.9462(4) | 0.25      | 0.0682(3) | 1.70(7)  |
| Si1               | 2e               | 0.5469(8) | 0.25      | 0.6118(6) | 1.88(9)  |
| Si2               | 2e               | 0.5554(8) | 0.25      | 0.260(7)  | 1.88(9)  |
| Si3               | 4f               | 0.7219(6) | 0.9997(6) | 0.8186(5) | 1.88(9)  |
| O1                | 4f               | 0.772(1)  | 0.092(1)  | 0.9691(9) | 2.0(1)   |
| O2                | 2e               | 0.780(1)  | 0.25      | 0.242(1)  | 2.0(1)   |
| O3                | 2e               | 0.094(2)  | 0.25      | 0.945(2)  | 2.0(1)   |
| O4                | 4f               | 0.894(1)  | 0.905(1)  | 0.794(1)  | 2.0(1)   |
| O5                | 2e               | 0.344(1)  | 0.25      | 0.665(2)  | 2.0(1)   |
| O6                | 2e               | 0.500(2)  | 0.25      | 0.4269(8) | 2.0(1)   |
| O7                | 4f               | 0.682(1)  | 0.1133(9) | 0.681(1)  | 2.0(1)   |
| O8                | 4f               | 0.544(1)  | 0.8961(9) | 0.8235(9) | 2.0(1)   |
| Na                | 4f               | 0.761(2)  | 0.935(1)  | 0.179(1)  | 10.7(3)  |
| O9 <sup>a,b</sup> | 2c               | 0.0       | 0.0       | 0.5       | 2.3(4)   |
| O10 <sup>a</sup>  | 2e               | 0.087(2)  | 0.25      | 0.460(2)  | 2.3(4)   |

<sup>a</sup> O9 and O10 oxygen atoms belong to water molecules. <sup>b</sup> Occupancy = 0.25.

**Table 3.** Selected Bond Distances (Å) and Angles (deg) for Na<sub>2</sub>H(NbO)Si<sub>4</sub>O<sub>11</sub>·1.25H<sub>2</sub>O

|           |               |           |               |
|-----------|---------------|-----------|---------------|
| Nb–O1     | 2.00(1) (×2)  | Si2–O2    | 1.65(1)       |
| Nb–O2     | 2.12(1)       | Si2–O6    | 1.61(1)       |
| Nb–O3     | 1.66(1)       | Si2–O8    | 1.620(9) (×2) |
| Nb–O4     | 2.062(9) (×2) | Si3–O1    | 1.56(1)       |
| Si1–O5    | 1.61(1)       | Si3–O4    | 1.55(1)       |
| Si1–O6    | 1.613(9)      | Si3–O7    | 1.59(1)       |
| Si1–O7    | 1.624(9) (×2) | Si3–O8    | 1.59(1)       |
| O1–Nb–O1  | 92.7(7)       | O7–Si1–O7 | 100.4(1)      |
| O1–Nb–O4  | 170.0(6) (×2) | O6–Si2–O8 | 105.0(8) (×2) |
| O2–Nb–O4  | 83.8(5) (×2)  | O1–Si3–O7 | 107.0(1)      |
| O5–Si1–O6 | 106.0(1)      | O4–Si3–O8 | 110.0(1)      |
| O6–Si1–O7 | 112.0(1) (×2) | O1–Nb–O3  | 98.0(1) (×2)  |
| O2–Si2–O8 | 107.6(9) (×2) | O2–Nb–O3  | 175.0(1)      |
| O1–Si3–O4 | 111.0(1)      | O4–Nb–O4  | 86.7(6)       |
| O4–Si3–O7 | 106.0(1)      | O8–Si2–O8 | 111.0(1)      |
| O1–Nb–O2  | 86.1(6) (×2)  | O2–Si2–O6 | 121.0(1)      |
| O1–Nb–O4  | 89.4(6) (×2)  | O1–Si3–O8 | 110.0(1)      |
| O3–Nb–O4  | 92.4(9) (×2)  | O7–Si3–O8 | 113.0(1)      |
| O5–Si1–O7 | 113.0(1) (×2) |           |               |

Si<sub>8</sub>O<sub>22</sub><sup>12-</sup>. The oxygen atoms of the silicate groups, O1, O4–(Si3), and O2(Si2), are linked to the niobium atoms. This linkage explains the <sup>29</sup>Si NMR shifts. Si3(2NbO, 2SiO) is at –86.4 ppm, Si2(1NbO, 3SiO) is at –92.9 ppm, and Si1(4SiO) is at –96.3 ppm. Because the ratio of silicon atoms is 2Si3:1Si2:1Si1, this assignment also accounts for the observed intensities. Silicon atom Si1 is connected to Si2 and Si3, through the O6 and O7

(28) Zah-Letho, J. J.; Jouanneaux, A.; Fitch, A. N.; Verbaere, A.; Tournoux, M. *Eur. J. Solid State Inorg. Chem.* **1992**, *29*, 1309.

(29) Crosnier, M. P.; Guyomard, D.; Verbaere, A.; Piffard, Y. *Eur. J. Solid State Inorg. Chem.* **1990**, *27*, 435.

(30) Galesic, N.; Brnicevic, N.; Matkovic, B.; Herceg, M.; Zelenko, B.; Slijkic, M. *J. Less-Common Met.* **1977**, *51*, 259.

**Table 4.** Fractional Atomic Coordinates and Isotropic Displacement Parameters ( $\text{\AA}^2$ ) for  $\text{HNb}(\text{H}_2\text{O})\text{Si}_4\text{O}_{11}\cdot\text{H}_2\text{O}$ 

| atom            | Wyckoff position | <i>x</i>  | <i>y</i>  | <i>z</i>  | <i>B</i> |
|-----------------|------------------|-----------|-----------|-----------|----------|
| Nb              | 2e               | 0.9109(4) | 0.25      | 0.0867(4) | 3.15(8)  |
| Si1             | 2e               | 0.572(1)  | 0.25      | 0.5845(9) | 3.2(1)   |
| Si2             | 2e               | 0.564(1)  | 0.25      | 0.258(1)  | 3.2(1)   |
| Si3             | 4f               | 0.7281(8) | 0.5045(8) | 0.8117(6) | 3.2(1)   |
| O1              | 4f               | 0.233(2)  | 0.907(2)  | 0.042(1)  | 3.0(1)   |
| O2              | 2e               | 0.746(2)  | 0.25      | 0.203(2)  | 3.0(1)   |
| O3              | 2e               | 0.065(2)  | 0.25      | 0.922(2)  | 3.0(1)   |
| O4              | 4f               | 0.910(2)  | 0.606(2)  | 0.825(1)  | 3.0(1)   |
| O5              | 2e               | 0.359(2)  | 0.25      | 0.561(2)  | 3.0(1)   |
| O6              | 2e               | 0.633(2)  | 0.25      | 0.429(1)  | 3.0(1)   |
| O7              | 4f               | 0.673(1)  | 0.105(1)  | 0.675(1)  | 3.0(1)   |
| O8              | 4f               | 0.549(2)  | 0.905(1)  | 0.802(1)  | 3.0(1)   |
| O9 <sup>a</sup> | 2c               | 0.0       | 0.0       | 0.5       | 12(1)    |

<sup>a</sup> O9 oxygen atom belongs to a water molecule

**Table 5.** Selected Bond Distances ( $\text{\AA}$ ) and Angles (deg) for  $\text{HNb}(\text{H}_2\text{O})\text{Si}_4\text{O}_{11}\cdot\text{H}_2\text{O}$ 

|           |                         |           |                         |
|-----------|-------------------------|-----------|-------------------------|
| Nb–O1     | 1.97(1) ( $\times 2$ )  | Si2–O2    | 1.59(2)                 |
| Nb–O2     | 1.88(2)                 | Si2–O6    | 1.58(1)                 |
| Nb–O3     | 2.20(2)                 | Si2–O8    | 1.63(1) ( $\times 2$ )  |
| Nb–O4     | 1.86(1) ( $\times 2$ )  | Si3–O1    | 1.61(1)                 |
| Si1–O5    | 1.52(2)                 | Si3–O4    | 1.60(1)                 |
| Si1–O6    | 1.68(1)                 | Si3–O7    | 1.60(1)                 |
| Si1–O7    | 1.62(1) ( $\times 2$ )  | Si3–O8    | 1.53(1)                 |
| O1–Nb–O1  | 91.0(1)                 | O7–Si1–O7 | 108.0(1)                |
| O1–Nb–O4  | 164.0(5) ( $\times 2$ ) | O6–Si2–O8 | 110.0(1) ( $\times 2$ ) |
| O2–Nb–O4  | 103.0(1) ( $\times 2$ ) | O1–Si3–O7 | 109.0(2)                |
| O5–Si1–O6 | 114.0(2)                | O4–Si3–O8 | 113.0(2)                |
| O6–Si1–O7 | 106.0(1) ( $\times 2$ ) | O1–Nb–O3  | 80.9(9) ( $\times 2$ )  |
| O2–Si2–O8 | 106.0(2) ( $\times 2$ ) | O2–Nb–O3  | 171.0(1)                |
| O1–Si3–O4 | 108.0(1)                | O4–Nb–O4  | 88.0(1)                 |
| O4–Si3–O7 | 115.0(1)                | O1–Si2–O2 | 106.4(9)                |
| O1–Nb–O2  | 93.0(1) ( $\times 2$ )  | O2–Si2–O6 | 108.0(2)                |
| O1–Nb–O4  | 87.8(9) ( $\times 2$ )  | O8–Si2–O8 | 117.0(1)                |
| O3–Nb–O4  | 83.3(9) ( $\times 2$ )  | O1–Si3–O8 | 106.0(1)                |
| O5–Si1–O7 | 112.0(1) ( $\times 2$ ) | O7–Si3–O8 | 106.0(1)                |

**Table 6.** Fractional Atomic Coordinates and Isotropic Displacement Parameters ( $\text{\AA}^2$ ) for  $\text{Cs}_{0.66}\text{H}_{0.33}\text{Nb}(\text{H}_2\text{O})\text{Si}_4\text{O}_{11}$ 

| atom            | Wyckoff position | <i>x</i>  | <i>y</i>  | <i>z</i>  | <i>B</i> |
|-----------------|------------------|-----------|-----------|-----------|----------|
| Nb              | 2e               | 0.9112(6) | 0.25      | 0.0779(5) | 4.5(2)   |
| Si1             | 2e               | 0.571(1)  | 0.25      | 0.585(1)  | 2.8(2)   |
| Si2             | 2e               | 0.549(1)  | 0.25      | 0.256(1)  | 2.8(2)   |
| Si3             | 4f               | 0.7318(9) | 0.5077(9) | 0.8139(8) | 2.8(2)   |
| O1              | 4f               | 0.242(2)  | 0.921(2)  | 0.037(1)  | 2.4(2)   |
| O2              | 2e               | 0.720(3)  | 0.25      | 0.187(2)  | 2.4(2)   |
| O3              | 2e               | 0.052(3)  | 0.25      | 0.891(2)  | 2.4(2)   |
| O4              | 4f               | 0.912(2)  | 0.619(2)  | 0.815(2)  | 2.4(2)   |
| O5              | 2e               | 0.345(2)  | 0.25      | 0.562(2)  | 2.4(2)   |
| O6              | 2e               | 0.650(3)  | 0.25      | 0.431(1)  | 2.4(2)   |
| O7              | 4f               | 0.683(2)  | 0.107(1)  | 0.680(1)  | 2.4(2)   |
| O8              | 4f               | 0.545(2)  | 0.909(1)  | 0.803(2)  | 2.4(2)   |
| Cs <sup>a</sup> | 2c               | 0.0       | 0.0       | 0.5       | 10.2(3)  |

<sup>a</sup> Occupancy = 0.66

atoms, respectively. In turn, Si2 is linked to Si3 through O8 (twice), and oxygen O5 is only linked to silicon atoms.

The niobium atom is found in oxidation state five, as was confirmed by magnetic moment measurements. Thus, the framework possesses a formal charge of  $-3$  per unit formula in the case of niobyl formation (compound **1**). This charge is balanced with the presence of one  $\text{Na}^+$  cation (two per unit formula) and a proton that presumably will be bonded to the free oxygen atom of the silicate anion forming a silanol group. The bond valence sum around the O5 atom is 1.04, supporting this hypothesis. In the acid phase (compound **2**), the niobyl group is absent, because of the protonation of the oxygen atom to form a water molecule. This results in a total charge  $-1$  for

**Table 7.** Selected Bond Distances ( $\text{\AA}$ ) and Angles (deg) for  $\text{Cs}_{0.66}\text{H}_{0.33}\text{Nb}(\text{H}_2\text{O})\text{Si}_4\text{O}_{11}$ 

|           |                         |           |                         |
|-----------|-------------------------|-----------|-------------------------|
| Nb–O1     | 2.04(2) ( $\times 2$ )  | Si1–O7    | 1.65(1) ( $\times 2$ )  |
| Nb–O2     | 1.99(2)                 | Si2–O2    | 1.59(2)                 |
| Nb–O3     | 2.33(2)                 | Si3–O8    | 1.55(1)                 |
| Nb–O4     | 1.84(1) ( $\times 2$ )  | Si2–O8    | 1.62(1) ( $\times 2$ )  |
| Si2–O6    | 1.63(2)                 | Si3–O1    | 1.60(1)                 |
| Si1–O5    | 1.62(2)                 | Si3–O4    | 1.66(2)                 |
| Si1–O6    | 1.75(2)                 | Si3–O7    | 1.61(1)                 |
| O1–Nb–O1  | 98.0(1)                 | O7–Si1–O7 | 103.0(1)                |
| O1–Nb–O4  | 169.0(1) ( $\times 2$ ) | O6–Si2–O8 | 113.0(2) ( $\times 2$ ) |
| O2–Nb–O4  | 102.0(2) ( $\times 2$ ) | O1–Si3–O7 | 110.0(2)                |
| O5–Si1–O6 | 118.0(2)                | O4–Si3–O8 | 113.0(2)                |
| O6–Si1–O7 | 104.0(1) ( $\times 2$ ) | O1–Nb–O3  | 83.0(1) ( $\times 2$ )  |
| O2–Si2–O8 | 99.0(2) ( $\times 2$ )  | O2–Nb–O3  | 163.0(7)                |
| O1–Si3–O4 | 114.0(1)                | O4–Nb–O4  | 80.0(1)                 |
| O4–Si3–O7 | 113.0(2)                | O1–Si2–O2 | 106.4(9)                |
| O1–Nb–O2  | 86.0(1) ( $\times 2$ )  | O2–Si2–O6 | 105.0(2)                |
| O1–Nb–O4  | 90.0(1) ( $\times 2$ )  | O8–Si2–O8 | 124.0(2)                |
| O3–Nb–O4  | 92.0(1) ( $\times 2$ )  | O1–Si3–O8 | 100.0(1)                |
| O5–Si1–O7 | 114.0(2) ( $\times 2$ ) | O7–Si3–O8 | 106.0(2)                |

**Table 8.** Interatomic Contacts Less than 3.6  $\text{\AA}$  for Atoms inside the Channel

|                  | 1                   |                         |                         | 2                      | 3                      |
|------------------|---------------------|-------------------------|-------------------------|------------------------|------------------------|
|                  | Na (4f)             | O9 (2c)<br>(occ = 0.25) | O10 (2e)                |                        |                        |
| O1               | 2.36(1)             |                         |                         |                        |                        |
| O2               | 2.92(1)             | 3.397(7) ( $\times 2$ ) | 2.63(2)                 |                        |                        |
| O3               | 2.37(1)             |                         |                         |                        |                        |
| O4               | 2.84(1)             | 2.993(9) ( $\times 2$ ) | 2.69(1) ( $\times 2$ )  | 3.52(1) ( $\times 2$ ) | 3.46(2) ( $\times 2$ ) |
| O5 <sup>a</sup>  | 2.40(1)             | 3.464(8) ( $\times 2$ ) | 2.33(2)                 | 3.39(1) ( $\times 2$ ) | 3.32(1) ( $\times 2$ ) |
| O6               |                     |                         | 3.03(2)                 | 3.42(1) ( $\times 2$ ) | 3.34(1) ( $\times 2$ ) |
| O7               |                     | 3.203(9) ( $\times 2$ ) |                         | 3.45(1) ( $\times 2$ ) | 3.43(1) ( $\times 2$ ) |
| O8               | 2.66(1),<br>3.26(1) |                         |                         |                        |                        |
| O9 <sup>b</sup>  | 3.08(1)             |                         | 2.408(5) ( $\times 2$ ) |                        |                        |
| O10 <sup>b</sup> |                     | 2.408(5) ( $\times 2$ ) |                         |                        |                        |
| Na               | 3.38(1)             | 3.08(1) ( $\times 2$ )  |                         |                        |                        |

<sup>a</sup> Oxygen atom only bonded a silicon atom. <sup>b</sup> O9 and O10 oxygen atoms belong to water molecules.

the framework that is balanced by the hydrogen atom of the silanol group. Finally, in the cesium phase (**3**) obtained from the acid form, two-thirds of the hydrogen atoms are substituted by cesium ions.

The  ${}^4\text{Si}_8\text{O}_{22}{}^{12-}$  anion has an approximately planar geometry and runs perpendicular to the *a* axis and parallel to the *b* axis (Figure 5). Niobium atoms running along the *b* axis join the silicate ribbons to form frameworks enclosing eight-sided (16 M–O atoms) and smaller six-sided (12 M–O) tunnels along the *b* axis. A structure plot of **1** showing the channels can be seen in Figure 6A. In the case of **2** and **3**, the channels are also present, but their shape is modified by the change in the geometry of the silicate anion (Figure 6B). In **1**, the channels are occupied by water molecules in two different crystallographic sites, 2e and 2c; the former is fully occupied, and the second one is partially occupied (occupancy factor 0.25). In the other two compounds, the channel is occupied only in the site 2c, fully with water in the case of **2**, and  $2/3$  with cesium ions for **3**. In **1**, a third site exists out of the channel that is fully occupied by the sodium ion in a general position 4f.

The 4f site is adequate for the occupation by a small cation such as  $\text{Na}^+$  but not enough for a large one like  $\text{Cs}^+$ . Furthermore, the 4f site seems to be stabilized where the silicate anion takes on a conformation in which oxygen atom O5 is closer to  $\text{Na}^+$  (2.40(1)  $\text{\AA}$ ). When the 4f site is empty, a different conformation is preferred, where the oxygen atom O5 moves toward the center of the larger channel where the water molecule (compound **2**) or Cs atom (compound **3**) is located.

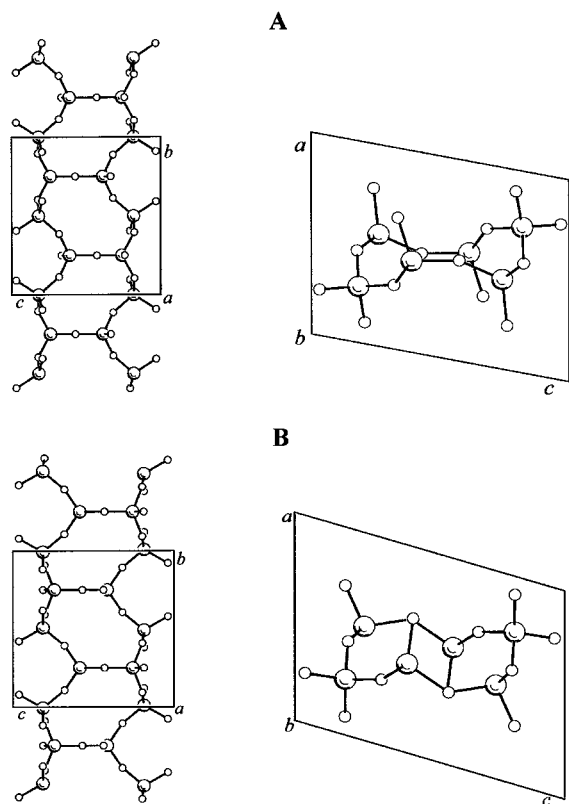


**Figure 5.** Structure of the  $\text{Si}_8\text{O}_{22}^{12-}$  anion in the compounds  $\text{Na}_2\text{H}(\text{NbO})\text{Si}_4\text{O}_{11}\cdot 1.25\text{H}_2\text{O}$  (A) and  $\text{Cs}_{0.66}\text{H}_{0.33}\text{Nb}(\text{H}_2\text{O})\text{Si}_4\text{O}_{11}$  (B).

The sodium ion is also close to oxygen atom O3, 2.37(1) Å, and has interatomic distances below 3.0 Å with four other oxygen atoms, O1, O2, O4, and O8. On the other hand, in the sodium phase, there are possible hydrogen bonds involving the two water molecules, 2.408(5) Å, and the water molecules and oxygen atoms belonging to the framework (O9 to O4 and O10 to O2, O4, and O5).

The three studied phases contained the same silicate anion:  $\text{Si}_8\text{O}_{22}^{12-}$ . According to the classification of Liebau,<sup>31</sup> this type of arrangement is called an “unbranched vierer double chain” and can be described by the following structural formula:  $\{\mathbf{uB}, 2_{\infty}1\}[^4\text{Si}_8\text{O}_{22}]^{12-}$ . As far as we know, this is the first description of this silicate anion type.

The only double silicate anion with an unbranched vierer double chain known at this moment is  $\text{Si}_8\text{O}_{20}^{8-}$ , which is present in narsarsukite,  $\text{Na}_4\text{Ti}_2[\text{Si}_8\text{O}_{20}]\text{O}_2$ .<sup>32</sup> Topologically, the new anion described in this work is equivalent to  $\text{Si}_4\text{O}_{11}^{6-}$ , present in the mineral kingdom (amphibole series), for example, in tremolite  $\text{Mg}_5\text{Ca}_2[\text{Si}_4\text{O}_{11}]_2(\text{OH})_2$  and anthophyllite  $(\text{Mg},\text{Fe})_7[\text{Si}_4\text{O}_{11}]_2(\text{OH})_2$ .<sup>33</sup> The difference between the two silicate anion types lies in the chain periodicity, two for the amphiboles and four in our compounds. In Figure 7, two representations of the silicate anion  $^2\text{Si}_4\text{O}_{11}^{6-}$  in tremolite are shown for comparison with the structure drawings for the silicate anion  $^4\text{Si}_8\text{O}_{22}^{12-}$  for the sodium (1) and cesium (3) phases shown in Figure 5. For the proton phase (2), the structure of the anion is similar to that of the cesium phase.

**Acknowledgment.** This work in Spain was supported by the Ministerio de Ciencia y Tecnología (BQU2000-0219 and

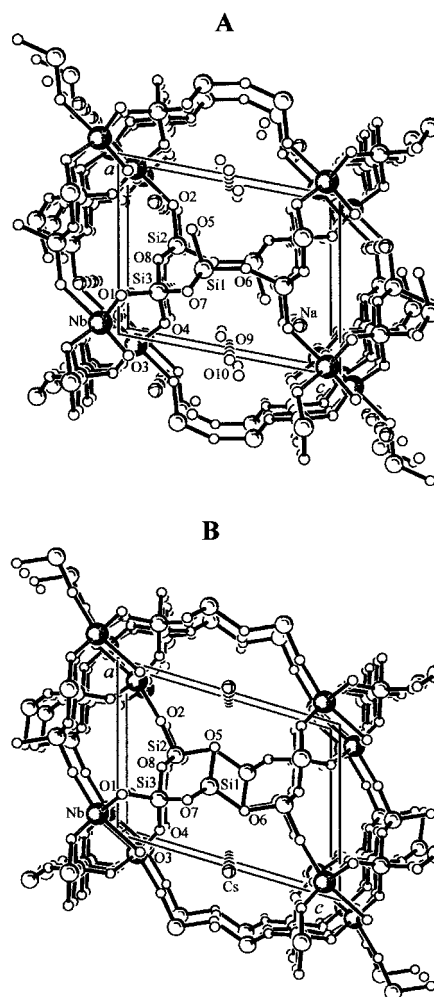


**Figure 6.** Channel structure of the compounds  $\text{Na}_2\text{H}(\text{NbO})\text{Si}_4\text{O}_{11}\cdot 1.25\text{H}_2\text{O}$  (A) and  $\text{Cs}_{0.66}\text{H}_{0.33}\text{Nb}(\text{H}_2\text{O})\text{Si}_4\text{O}_{11}$  (B) along [101]. The origin of the cell is shown in the left lower corner.

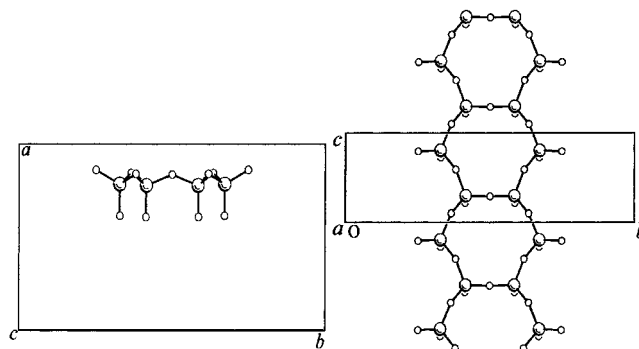


**Figure 7.** Longitudinal and lateral views of the structure of the  $\text{Si}_4\text{O}_{11}^{6-}$  anion in tremolite (amphiboles group).

MAT2000-1654). A.C. and A.B. gratefully acknowledge Lockheed-Martin Energy Systems, Inc., through Grant No. 9800585 and Oak Ridge National Laboratory for financial support through the Energy Management Science Program (EMSP).

**Supporting Information Available:** X-ray crystallographic file, in CIF format. This material is available free of charge via the Internet at <http://pubs.acs.org>.

(31) Liebau, F. *Structural Chemistry of Silicates*; Springer-Verlag: Berlin, Heidelberg, 1985.

(32) Peacor, D. R.; Buerger, M. J. *Am. Mineral.* **1962**, *47*, 539.

(33) Hawthorne, F. C.; Grundy, H. D. *Can. Mineral.* **1976**, *14*, 334.